Magnetotransport studies on the Ruddlesden Popper phases $Sr_2RMn_2O_7$ (R = Nd, Pr, Ho, Y) and $Sr_{2-x}Nd_{1+x}Mn_2O_7$ (x = 0, 0.1, 0.2, 0.5)

1999 J. Phys.: Condens. Matter 11 9053

(http://iopscience.iop.org/0953-8984/11/46/308)

J. Phys.: Condens. Matter **11** (1999) 9053–9072. Printed in the UK PII: S0953-8984(99)05050-X

Magnetotransport studies on the Ruddlesden Popper phases $Sr_2RMn_2O_7$ (R = Nd, Pr, Ho, Y) and $Sr_{2-x}Nd_{1+x}Mn_2O_7$ (x = 0, 0.1, 0.2, 0.5)

A I Coldea, L E Spring, S J Blundell, J Singleton and W Hayes
Clarendon Laboratory, University of Oxford, Parks Road, Oxford OX1 3PU, UK

Received 3 June 1999

Abstract. We study effects on magnetotransport produced by changing the size of the trivalent ions R^{3+} in the layered polycrystalline materials $Sr_2RMn_2O_7$ (R = Pr, Nd, Ho, Y) and by varying the mixed-valence ratio Mn^{3+}/Mn^{4+} in the series $Sr_{2-x}Nd_{1+x}Mn_2O_7$ ($x = 0, 0.1, 0.2, 0.5$). The results of our magnetic and electrical measurements are related to the measured structural characteristics of each compound. For the $Sr_2RMn_2O_7$ series, colossal magnetoresistance (CMR) is observed below 150 K for R = Pr and R = Nd but not for samples containing R = Ho or R = Y ions, which have smaller ionic radii. For R = Ho and R = Y, the absence of CMR is correlated with the paramagnetic and insulating properties of the samples. Within the series $Sr_{2-x}Nd_{1+x}Mn_2O_7$, the CMR effect is also observed for temperatures below 150 K and increases as the temperature decreases. In this series the samples show a mixture of spin-glass and antiferromagnetic behaviour ($x = 0, 0.1$) or no long-range magnetic order ($x = 0.2, 0.5$). The largest CMR at high temperatures (above 100 K) and high magnetic fields (14 T) is observed for the $x = 0.2$ sample, which also shows the largest magnetization per formula unit. The observed CMR in the compounds studied here is attributed to magnetic cluster formation.

(Some figures in this article appear in colour in the electronic version; see `www.iop.org`)

1. Introduction

There has been much recent interest in the unusual magnetotransport properties of the Ruddlesden Popper (RP) phases $(A, R)_{n+1}Mn_nO_{3n+1}$ where A and R are a divalent and a trivalent cation, respectively, and n represents the number of layers of vertex-shared MnO_6 octahedra stacked along the crystallographic direction [001] (see figure 1(a) in section 3). It has been shown that several stoichiometries, in particular those belonging to the $n = 2$ [1–3] and $n = \infty$ [4–7] series, display colossal magnetoresistance (CMR). Their resistivity can change by a factor of 10^2 to 10^5 with applied magnetic field [8, 9] and this greatly exceeds the so-called *giant* values observed in magnetic multilayers [10].

Much of the experimental and theoretical work has focused on the so-called infinite-layer ($n = \infty$) mixed-valence manganese perovskites (A, R)MnO_3 [11, 12], although Mn-containing pyrochlores [13, 14] and Cr chalcogenide spinels [15] have also displayed CMR phenomena in the absence of mixed valence. In all of these cases, the CMR effect is observed close to the transition temperature between a paramagnetic-like state and a ferromagnetically ordered state. Similar behaviour has been observed in $Sr_{1.8}La_{1.2}Mn_2O_7$, which undergoes a metal–insulator transition at its Curie temperature; it shows CMR at this temperature, much larger than that observed in the perovskite, $Sr_{0.4}La_{0.6}MnO_3$, which has a similar concentration of Mn^{3+} and Mn^{4+} [3, 6].

0953-8984/99/469053+20$30.00

In contrast, it has been shown recently that CMR in $Sr_2NdMn_2O_7$ and $Sr_{1.9}Nd_{1.1}Mn_2O_7$ is not associated with bulk three-dimensional ferromagnetic order [16], which suggests that besides the double-exchange mechanism [17], expected as a result of the mixed valence, there are other possible contributions to the CMR effect. In this paper we concentrate on these two compounds and six others which are also members of the $n = 2$ series, described by the general formula $(A, R)_3Mn_2O_7$. The reduction in dimensionality on moving from the infinite-layer to the $n = 2$ systems gives rise to a relatively narrow electronic bandwidth in which the carriers are susceptible to strong electron correlation effects and anisotropy of the electrical and magnetic interactions [3, 18]. Theoretical work on a range of CMR materials [19] has shown that there are strong correlations between electronic motion and the lattice which can result in the formation of ferromagnetic clusters or magnetic polarons [20–23]. Furthermore, the presence of the Jahn–Teller ion, Mn^{3+}, in the mixed-valence systems changes the magnetic anisotropy by increasing the $d_{3z^2-r^2}$ character in the occupied e_g state, thus affecting charge transport as well [24, 25].

The aim of this paper is to interpret the changes in magnetotransport data of the $n = 2$ $(Sr, R)_3Mn_2O_7$ series either as a function of the size of the trivalent cation dopant (R = Pr, Nd, Ho, Y), in the case where the Mn^{3+}/Mn^{4+} ratio is unity, or by varying the mixed-valence Mn^{3+}/Mn^{4+} ratio by changing x in the series $Sr_{2-x}Nd_{1+x}Mn_2O_7$ ($x = 0$, 0.1, 0.2, 0.5). The results are discussed in the light of previous information obtained from neutron diffraction, magnetization and resistivity measurements on the same compounds.

2. Experimental procedure

Polycrystalline samples were synthesized by firing stoichiometric quantities of dried R_2O_3 (Pr_6O_{11} in the case of $Sr_2PrMn_2O_7$), $SrCO_3$ and MnO_2 in alumina crucibles at temperatures between 800 °C and 1500 °C. The precise synthesis conditions for the $Sr_{2-x}Nd_{1+x}Mn_2O_7$ and $Sr_2RMn_2O_7$ phases together with their structural characterization by powder neutron diffraction experiments are described in detail elsewhere [26–29]. The $Sr_2PrMn_2O_7$ sample was characterized only by powder x-ray diffraction using a Siemens D5000 diffractometer. The ease of preparation of single-RP-phase materials is partially determined by the degree of cation ordering, i.e. by the tendencies of the smaller cations to occupy the smaller nine-coordinate rock-salt site and the larger cations to occupy the twelve-coordinate perovskite block site [26]. The oxygen deficiency obtained by iodometric titration in the compounds studied, $(A, R)_3Mn_2O_{7-\delta}$, was less than 0.04 ($\delta < 0.04$). The oxidation states of Mn ions are given in the following section in table 1.

Magnetization measurements were carried out using a Quantum Design MPMS SQUID Magnetometer with typically 20–100 mg samples mounted in gelatin capsules. The magnetic susceptibilities were measured in the temperature range $T = 5$–300 K and in fields of $B = 0.01$–0.1 T. Data were collected after cooling the sample in the absence of an applied magnetic field (zero-field cooled, ZFC) and after cooling the sample in a measuring field, typically 0.01 or 0.05 T (field cooled, FC). High-field magnetization measurements in magnetic inductions of up to 15 T were performed using an extraction magnetometer inserted in a 17 T superconducting magnet.

Magnetotransport measurements were carried out on sintered bars (typically $2 \times 2 \times 5\,mm^3$) using a DC four-terminal method with the current (<50 μA) perpendicular to the magnetic field. Gold pads were evaporated onto the bars prior to attaching the Cu wires with Ag epoxy. Resistivity was measured as a function of temperature ($T = 4$–300 K) whilst cooling in zero field and for temperatures $T = 4$–250 K whilst warming in fields of 14 T. The field dependence of the resistivity was measured between 0 T and 14 T at constant temperature and

compared with the field dependence of the magnetization measured at the same temperature. Magnetoresistance is defined as MR (%) $= -[(\rho(B) - \rho(0))/\rho(0)] \times 100$, where $\rho(B)$ is the resistivity in a magnetic field B and $\rho(0)$ is the resistivity in zero applied field.

3. Results and discussion

3.1. Structural properties of the $Sr_2RMn_2O_7$ and $Sr_{2-x}Nd_{1+x}Mn_2O_7$ series

In the $n = 2$ layered structure the perovskite slabs, composed of two layers of MnO_6 octahedra, are separated by a layer of ((A/R), O) cations and anions which adopt the rock-salt structure (see figure 1(a)).

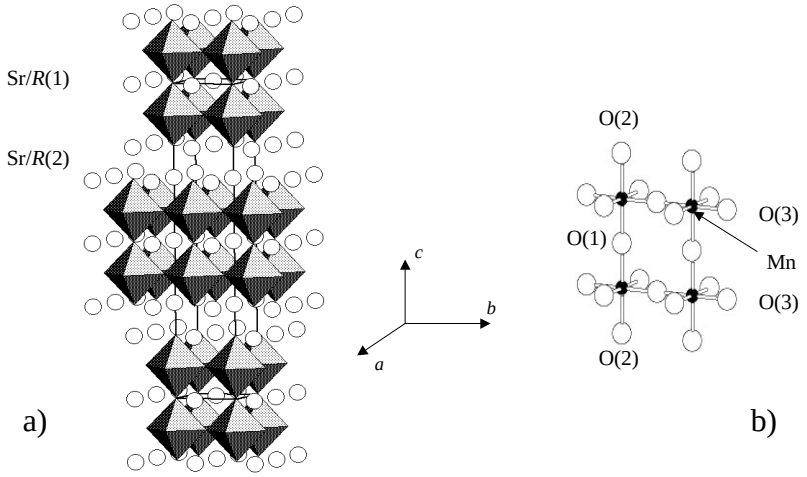

Figure 1. (a) The tetragonal crystal structure of the $n = 2$ Ruddlesden Popper $Sr_2RMn_2O_7$ compound showing MnO_6 octahedra and Sr/R ions as empty circles. (b) The Mn–O(1) and Mn–O(2) out-of-plane bond as well as and Mn–O(3) in-plane bond length.

The structural parameters of the two series of compounds $Sr_2RMn_2O_7$ (R = Pr, Nd, Y, Ho) and $Sr_{2-x}Nd_{1+x}Mn_2O_7$ ($x = 0$, 0.1, 0.2, 0.5) are listed in table 1. In the present study, the samples are either a single-phase $n = 2$ RP material contaminated by a small amount of $n = \infty$ RP (<7%) for R = Ho, Y and Nd ($x = 0.2$ and $x = 0.5$) or two discrete $n = 2$ RP phases with slightly different lattice parameters for R = Pr and R = Nd with $x = 0$ and $x = 0.1$. The ratio between the two phases is 65.2/35.2 for $x = 0$ and 46/54 for $x = 0.1$ (see table 1). Because of the close similarity in lattice parameters for the biphasic compounds, some of the structural parameters are taken to be average values in order to allow comparison with other quantitative coefficients.

The space group used in the Rietveld refinement of the neutron data was the tetragonal $I4/mmm$ group. However, for R = Ho and Y, the MnO_6 octahedra are allowed more freedom both in terms of orientation and the number of independent Mn–O bond lengths in order to satisfy the coordination requirements of the nine-coordinate site; the space group used in these two cases was $P4_2/mnm$ [27]. The out-of-plane Mn–O bond length (see figure 1(a)) of the $Sr_2RMn_2O_7$ structure is particularly sensitive to elongation in the presence of Jahn–Teller Mn^{3+} (d^4) ions [27, 30]. This may result in part from the additional flexibility in the $n = 2$ tetragonal systems for the out-of-plane Mn–O bonds (see figure 1(b)) to extend into the rock-salt layer, the nine-coordinate site of which is preferentially occupied by the A-site

Table 1. Structural parameters of the compounds studied. The ratio of Mn^{3+}/Mn^{4+} is obtained considering the oxygen deficiency δ in the formula $(A, R)_3Mn_2O_{7-\delta}$; the ⟨Mn–O⟩ apical bond is calculated as the average of the apical bonds (see figure 1(b)). Δ is defined as the ratio of the averaged out-of-plane (apical) to the in-plane Mn–O bond length.

Compounds	a (Å)	c (Å)	Mn^{3+}/Mn^{4+}	⟨Mn–O⟩ (Å)	Δ	$n = \infty$ (%) RP phases
$Sr_2YMn_2O_7$	5.4045(6)	19.9054(2)	1.04	1.995	1.044	2.2(1)
$Sr_2HoMn_2O_7$	5.4038(5)	19.9050(2)	1.04	1.996	1.045	3.0(2)
$Sr_2NdMn_2O_7$ (65%)	3.8490(6)	19.9599(7)	1.17	1.963	1.021	—
$Sr_2NdMn_2O_7$ (35%)	3.8451(1)	20.0222(1)	1.17	1.963	1.021	—
$Sr_{1.9}Nd_{1.1}Mn_2O_7$ (46%)	3.8456(6)	20.0266(6)	1.27	1.971	1.025	—
$Sr_{1.9}Nd_{1.1}Mn_2O_7$ (54%)	3.8421(7)	20.0831(7)	1.27	1.971	1.025	—
$Sr_{1.8}Nd_{1.2}Mn_2O_7$	3.8399(7)	20.1457(4)	~ 1.56	1.993	1.039	6.8(6)
$Sr_{1.5}Nd_{1.5}Mn_2O_7$	3.8367(1)	20.3084(6)	3.54	2.040	1.064	4.6(7)

cation with the smaller radius [27]. For example, in $Sr_2HoMn_2O_7$ and $Sr_2YMn_2O_7$ this site is preferentially occupied by Ho^{3+} and Y^{3+} cations, thus facilitating elongation of the out-of-plane (apical) bonds, and reducing the bandwidth associated with the e_g electrons. In the Pr and Nd samples the similarity in site radii for the nine- and twelve-coordinate sites is reflected in the minimal structural distortion relative to the Ho and Y phases [27].

Table 1 also shows the variation of structural parameters for the series $Sr_{2-x}Nd_{1+x}Mn_2O_7$ as the concentration of electrons in the e_g orbitals increases (hole doping decreases) with increasing Nd concentration x. Considering the averaged values of bond lengths for biphasic compounds (the two phases have very similar lattice parameters), we can define the distortion parameter of MnO_6 octahedra (Jahn–Taller distortion) Δ for a two-dimensional system as the ratio of the averaged out-of-plane Mn–O to the in-plane Mn–O bond length [31]. With increasing x or decreasing hole doping, the lattice parameter a decreases and the c-value increases. Also, the decrease in hole doping from $x = 0$ to $x = 0.5$ is consistent with the increase in the Jahn–Teller distortion Δ as observed in other layered manganites [24]. This is expected to influence the magnetic and electrical properties of the materials (see the following sections). The lengthening of the out-of-plane Mn–O bonds will reduce the coupling between bilayers as well as that between the two layers comprising a bilayer, therefore strengthening the two-dimensional nature of the structure [16, 28, 29]. A more detailed discussion of structural parameters is given in references [16, 30].

3.2. Magnetotransport properties

3.2.1. $Sr_2RMn_2O_7$ (R = Pr, Nd, Y, Ho). For the $Sr_2RMn_2O_7$ (R = Pr, Nd, Ho, Y) series the ratio between the Mn^{4+}- and Mn^{3+}-ion concentration is approximately unity; deviations from unity are explained by slight oxygen non-stoichiometry (see table 1). Changes in the magnetotransport behaviour can then be attributed to the variation in the mean radius of the R^{3+} ion. This modification will change the lattice constants and consequently the electronic bandwidth of e_g electrons. In the following discussion we look at the changes in the magnetic and electrical properties of these compounds as a result of varying the size of R^{3+}.

Magnetization measurements as a function of temperature in a field of 0.05 T for the $Sr_2RMn_2O_7$ (R = Pr, Nd, Y, Ho) compounds are shown in figure 2. There is a large divergence between zero-field-cooled (ZFC) and field-cooled (FC) magnetization curves for R = Pr and Nd. The shape of the curves indicates a complex behaviour for these two samples resulting not only from the competing ferromagnetic and antiferromagnetic exchange interactions present

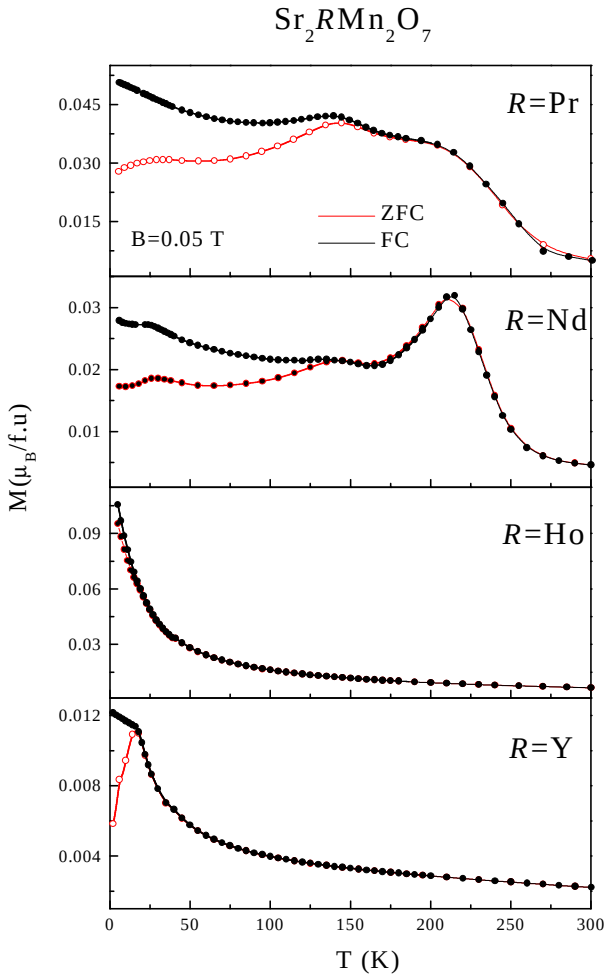

Figure 2. Magnetization measurements as a function of temperature for $Sr_2RMn_2O_7$ (R = Pr, Nd, Ho, Y) in a field of 0.05 T. The empty circles represent zero-field-cooled magnetization data (ZFC) and full circles represent field-cooled (FC) data.

for mixed-valence states of manganese but also from the presence of two discrete phases (see table 1). Previous neutron diffraction measurements on the biphasic $Sr_2NdMn_2O_7$ sample [16] suggested that the magnetic behaviour is different in the two phases; manganese magnetic moments are antiferromagnetically aligned in the majority phase ($T_N = 140$ K), whereas the minority phase is a spin glass with $T_{sg} < 50$ K. Nd moments order antiferromagnetically only below 30 K and in the intermediate region ($T = 30$–140 K) are frozen in a spin-glass-like fashion, thus contributing to the hysteresis in the magnetization. It was suggested that the peak in the magnetization around 210 K is caused by the formation of superparamagnetic or small ferromagnetic clusters [30]. For the biphasic Pr sample no powder neutron diffraction data are available to test for the presence of antiferromagnetic order. However, their structural similarities with the Nd sample (atomic radii) and the magnetization data (figure 2) suggest that the magnetic interactions may be very similar. The maximum in magnetization at 143 K in $Sr_2PrMn_2O_7$ could be due to the onset of antiferromagnetic order in one of the two constituent

phases, whereas the reduction of ZFC magnetization indicates either a spin-glass freezing or antiferromagnetic order of the Pr moments by analogy with the behaviour of the $Sr_2NdMn_2O_7$ compound.

In contrast, neutron diffraction studies on $Sr_2HoMn_2O_7$ and $Sr_2YMn_2O_7$ showed no long-range magnetic order [27] and magnetization data shown in figure 2 followed a paramagnetic behaviour to low temperatures. The divergence between the ZFC and FC magnetization at 42 K for the Ho sample and at 17 K for Y has been attributed to spin-glass freezing of the manganese moments arising both from competing exchange interactions and disorder in the spatial location of Mn^{3+} and Mn^{4+} [30]. The non-magnetic character of Y^{3+} ions means that only the manganese ions can contribute to the low-temperature spin-glass-like behaviour observed in the $Sr_2YMn_2O_7$ compound. The effective magnetic moments of manganese for the Y and Ho samples agree fairly well with those calculated on the basis of a simple, non-interacting-ion model by fitting with a Curie–Weiss law at high temperatures† whereas the susceptibility data for the Pr and Nd compounds could not be described by a Curie–Weiss law in any region of the temperature range studied.

The temperature dependences of the resistivity in zero applied field and at 14 T for $Sr_2RMn_2O_7$ (R = Pr, Nd, Y, Ho) are shown in figure 3. As in the case of the magnetization, the resistivity for samples with smaller ions (e.g. Y and Ho) behaves differently from that of the compounds with larger ions (e.g. Pr and Nd). The resistivity of R = Ho and R = Y samples is strongly activated, increasing exponentially as temperature decreases, and at low temperatures the resistivity increases beyond the measuring range. In addition, a field of 14 T has a much smaller effect compared to the case of the Pr and Nd samples.

The maximum resistivity of the Nd sample reaches a value of $1 \times 10^7\ \Omega$ cm whereas for the Pr sample the maximum resistivity is nearly three orders of magnitude lower, i.e. $4 \times 10^4\ \Omega$ cm‡. Overall, the temperature dependence of the resistivity for the Pr and Nd samples seems to be characterized by three different regions: the high-temperature region which shows an insulating behaviour (above $T = 200$ K for the Pr sample and above $T = 150$ K for the Nd sample), the intermediate-temperature region $T = 50$–150 K where the resistivity slope, $d\rho/dT$, decreases and the low-temperature region (below 50 K) where $d\rho/dT$ increases much more abruptly than in the first region. The increase in resistivity at low temperature could be connected with the ordering of the Nd and Pr moments below 50 K [1] or may be due to Anderson localization of the charge carriers as proposed for the layered manganite with R = La [33]. On the application of a magnetic field of 14 T, the MR values (as defined in section 2) were 24% for the Ho sample at 125 K and 32% for the Y sample at 100 K. In comparison, the resistivity of the Nd and Pr samples decreases by a few orders of magnitude in the same applied field. A change in the slope of the resistivity, reminiscent of a metal–insulator transition, is observed in 14 T at 80 K for the Pr sample and at about 75 K for the Nd sample.

3.2.2. $Sr_{2-x}Nd_{1+x}Mn_2O_7$ ($x = 0$, 0.1, 0.2, 0.5). In the case of the $Sr_{2-x}Nd_{1+x}Mn_2O_7$ ($x =$ 0–0.5) series it is of interest to observe the effects of band filling upon magnetic properties when the relative concentrations of Mn^{3+}/Mn^{4+} ions are varied. Figure 4 shows magnetization as a function of temperature for these compounds in a field of 0.05 T for the samples with

† The Curie–Weiss law applies over a wider temperature range ($T = 124$–300 K) for the Ho sample than for the Y sample ($T = 240$–300 K).

‡ A similar difference in the maximum the resistivity was found for the $n = \infty$ RP phases $Sr_{0.5}R_{0.5}MnO_3$ (R = Pr and Nd). These have similar concentrations of mixed-valence ions Mn^{3+} and Mn^{4+} to the compounds studied in this case. The difference between their resistivity values was assigned to their difference in magnetic structure in the low-temperature region (A-type antiferromagnetic order for $Sr_{0.5}Pr_{0.5}MnO_3$ and CE-type (charge-ordering) antiferromagnetic order for $Sr_{0.5}Nd_{0.5}MnO_3$ [32]).

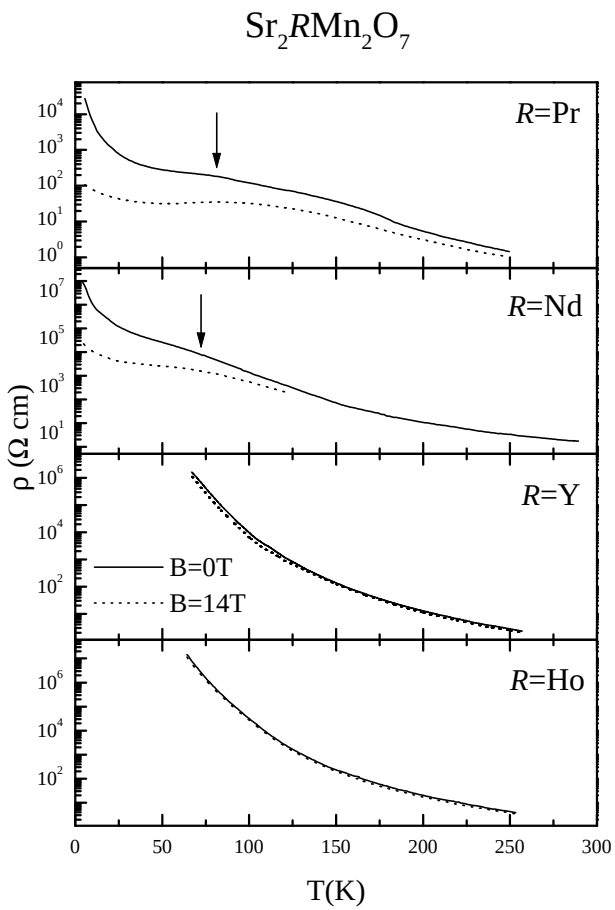

Figure 3. The temperature dependence of the resistivity in zero field (solid line) and 14 T (dotted line) for the series $Sr_2RMn_2O_7$ (R = Pr, Nd, Ho, Y). The arrows indicate the position of peaks where $d\rho/dT$ changes slope.

$x = 0, 0.1$ and in a field of 0.01 T for the samples with $x = 0.2, 0.5$. As seen previously for the $Sr_2NdMn_2O_7$ compound, the temperature dependence of the magnetization is complex; this is due not only to the competition between the ferromagnetic and antiferromagnetic interactions between the Mn ions but also to the presence of Nd ions which order antiferromagnetically at low temperatures [16]. There is a divergence between the ZFC and FC curves which occurs at 260 K for $x = 0.2$ and $x = 0.5$ in an applied field of 0.01 T and below 140 K for $x = 0$ and $x = 0.1$ samples in 0.05 T. The local maximum observed at approximately 210 K in the $Sr_2NdMn_2O_7$ sample is not seen for finite x. In earlier studies, the appearance of successive maxima in the magnetization of $x = 0, 0.1$ was attributed to the presence of the two distinct magnetic phases. In view of the multiple peaks also shown by the single-phase $n = 2$ RP $x = 0.2$ and $x = 0.5$ samples, this explanation is now thought unlikely to be true. This suggestion is supported by complex and highly anisotropic behaviour of the magnetization reported for single crystals of $Sr_{1.5}Nd_{1.5}Mn_2O_7$ and $Sr_{1.5}Pr_{1.5}Mn_2O_7$ [34]; in these cases the ferromagnetic ordering was observed at 280 K and the onset of antiferromagnetic correlations at 100 K. All of these compounds, including our single-phase $x = 0.2$ and $x = 0.5$ materials, exhibit successive maxima in magnetization, suggesting that this behaviour

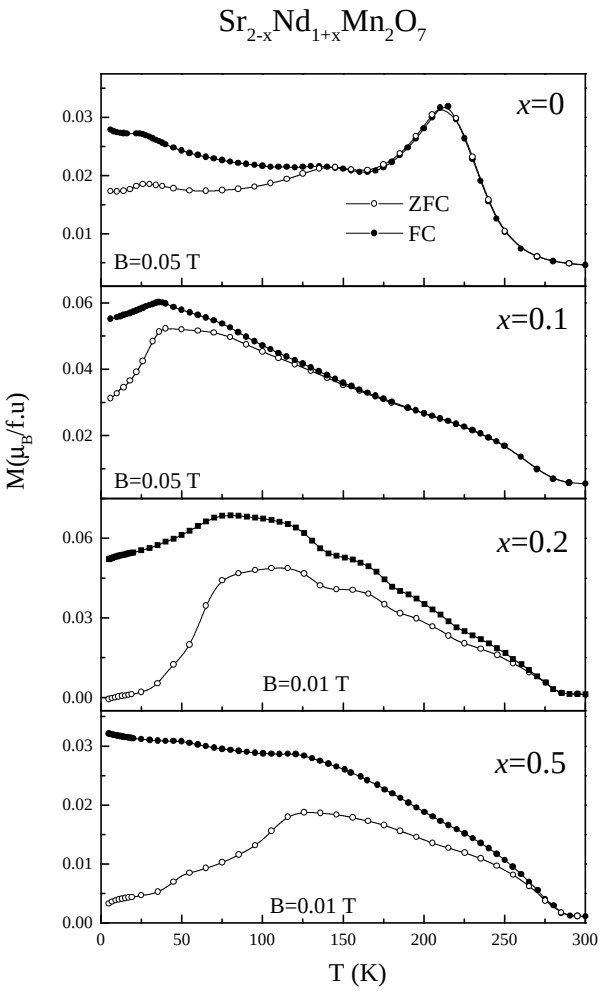

Figure 4. Magnetization measurements as a function of temperature for $Sr_{2-x}Nd_{1+x}Mn_2O_7$ ($x = 0$, 0.1, 0.2, 0.5) compounds in a field of 0.05 T for the $x = 0$ and $x = 0.1$ compounds and 0.01 T for $x = 0.2$ and $x = 0.5$. The full circles represent field-cooled (FC) data and empty circles represent zero-field-cooled (ZFC) data.

is perhaps an intrinsic characteristic of these materials in which competing antiferromagnetic and ferromagnetic interactions occur.

Previous neutron diffraction measurements for $x = 0.2$ [28] and $x = 0.5$ compounds [29] did not reveal any long-range magnetic order, in contrast to the observation of antiferromagnetism in the majority phases of the $x = 0$ and $x = 0.1$ materials [16]. In each case the increase in magnetization on cooling between 300 K and 250 K, as seen in figure 4, suggests the formation of regions of ferromagnetic spin correlation. The absolute value of the magnetization per formula unit suggests that the ferromagnetic clusters have the largest concentration for the $x = 0.2$ composition. Because of the lack of a bulk ferromagnetic phase in any of these four samples, it is likely that any spin correlations are on a local scale and/or are restricted to two-dimensional ordering within the perovskite bilayers.

The temperature dependence of the resistivity of the $Sr_{2-x}Nd_{1+x}Mn_2O_7$ series is shown

in figure 5. The resistivity shows an insulating behaviour over the entire temperature range except for the composition $x = 0.2$ where it levels off at 1×10^3 Ω cm below 75 K†. Similar behaviour was also observed for $x = 0.3$ and $x = 0.4$ [35].

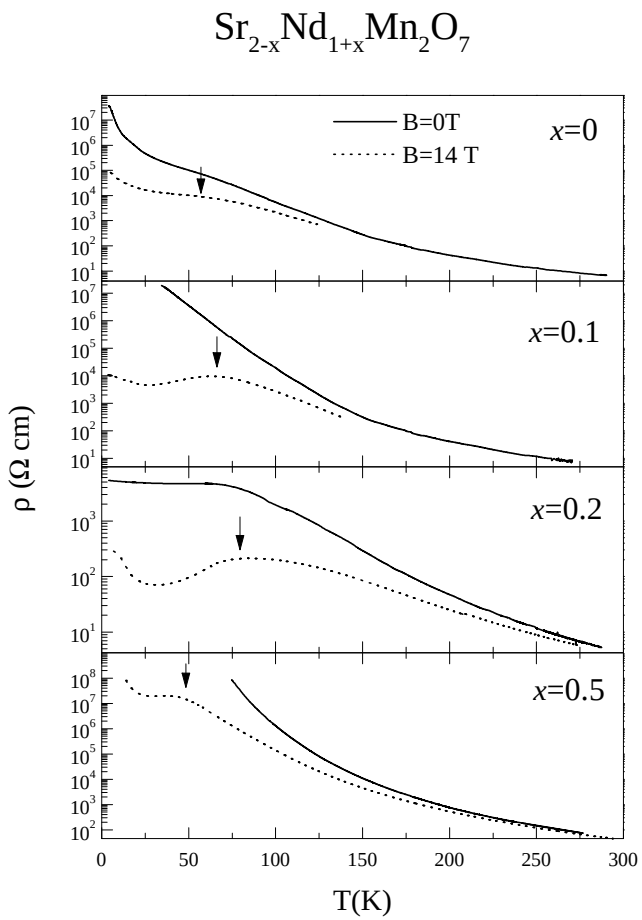

Figure 5. The temperature dependence of the resistivity in zero field (solid line) and 14 T (dashed line) for the series $Sr_{2-x}Nd_{1+x}Mn_2O_7$ ($x = 0$, 0.1, 0.2, 0.5). The arrows indicate the position of the peaks where $d\rho/dT$ changes slope.

The reason for low-temperature saturation of resistivity at these concentrations is at present unclear. The other samples have maximum, measurable values of resistivity in zero field of the order of 1×10^7 Ω cm which are dramatically reduced in the presence of a magnetic field. On applying a magnetic field of 14 T, the resistivity decreases strongly below 150 K for all samples and a peak reminiscent of the metal–insulator transitions seen in perovskite CMR materials [6] is induced between 50–100 K, followed at $T < 50$ K by a second insulating region as described above. The local maxima which appear for all compositions in 14 T are observed at approximately 75 K for the $x = 0$, $x = 0.1$ and 0.2 compounds and at 50 K for $x = 0.5$.

† Two different samples with slightly different concentrations of the $n = \infty$ RP phase were measured and they show similar behaviour.

3.3. Magnetoresistance of $Sr_{1.8}Nd_{1.2}Mn_2O_7$ and $Sr_{1.5}Nd_{1.5}Mn_2O_7$

We now consider the two samples which consist mainly of an $n = 2$ RP single phase and we try to establish the possible mechanisms which contribute to magnetoresistance values and the relationship between the magnetoresistance and magnetization.

The field dependences of the magnetization and resistivity of the two single-phase compounds $x = 0.2$ and $x = 0.5$ are shown in figures 6(a) and 6(b). In the high-temperature region the linear field dependence of the magnetization up to 15 T suggests a

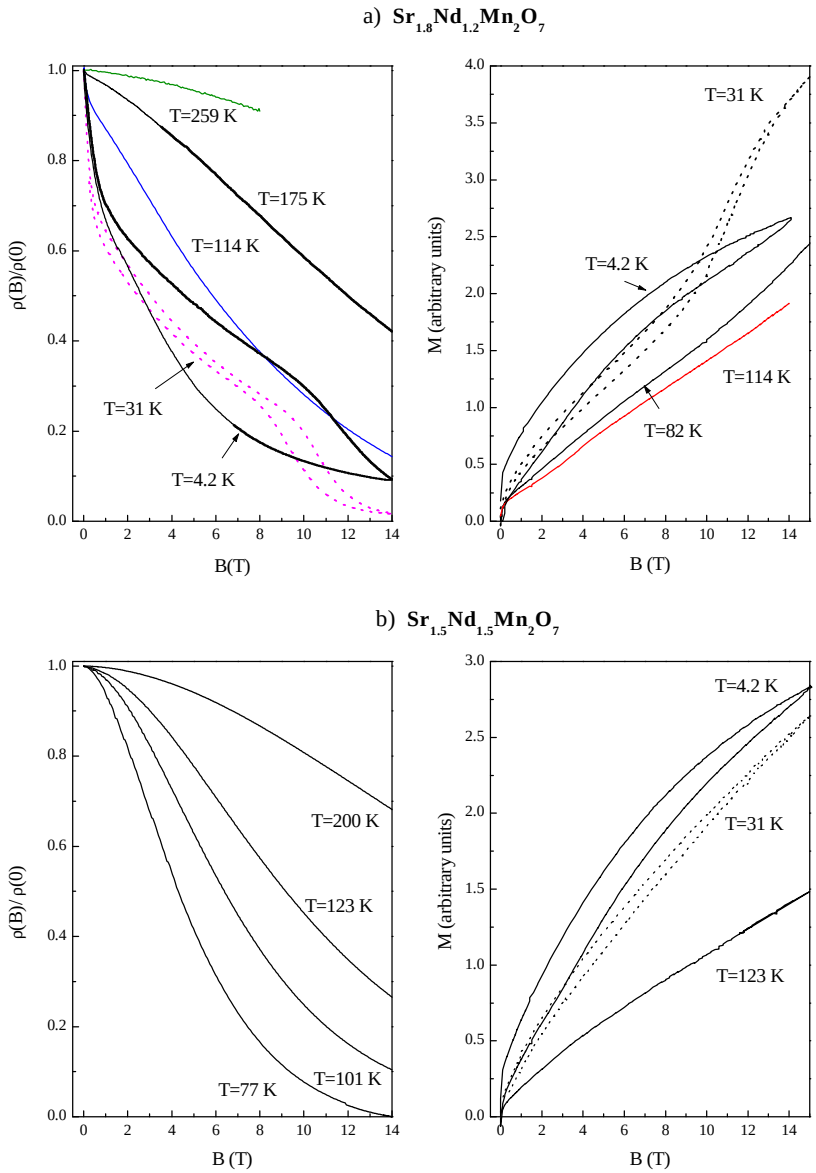

Figure 6. The field dependence of the magnetization and the resistivity at constant temperatures for (a) $Sr_{1.8}Nd_{1.2}Mn_2O_7$ and (b) $Sr_{1.5}Nd_{1.5}Mn_2O_7$.

paramagnetic-like behaviour for both samples, as is also observed in SQUID data at lower magnetic fields [30]. However, the temperature dependence of the magnetic susceptibility failed to fit a Curie–Weiss model, perhaps suggesting the presence of magnetic polarons as seen for the perovskite $(La–Y/Tb)_{2/3}Ca_{1/3}MnO_3$ [21]. On lowering the temperature, the field dependence of the magnetization for the $x = 0.2$ sample changes slope above 10 T at 31 K, indicating changes in the magnetic structure at low temperatures and in high magnetic fields. These changes could be connected with the changes in the balance between the ferromagnetic and antiferromagnetic interactions due to the influence of Nd moments. Nd moments were found to order antiferromagnetically below 30 K for $x = 0$ and $x = 0.1$ [16]. The strong frustration of the magnetic ions at low temperatures could also explain the observed hysteresis between the up and down sweep. The magnetic fields used in these experiments are still probably relatively small compared to those necessary to align all of the spins (e.g. a field of 25 T was necessary to reach saturation in $Nd_{0.5}Ca_{0.5}MnO_3$ at 4 K [36]).

The field dependence of the resistivity normalized to the zero-field value for the samples with $x = 0.2$ and $x = 0.5$ seems to be very well correlated with the changes in the magnetic structure (figure 6). On increasing the temperature, the field dependence of the resistivity changes its shape from concave to convex and this could be associated with the changes in the magnetic state (from a complex magnetic state at low temperature to a disordered state at high temperature [37]). At low temperatures ($T \leqslant 31$ K), the resistivity of the $x = 0.2$ sample shows hysteresis between the up and down sweep which is clearly associated with the hysteresis observed in magnetization measurements. Another feature observed for both the resistivity and magnetization is the anomaly at 31 K above 8 T which suggests that the changes in the magnetic interactions between the Mn ions (perhaps on antiferromagnetic ordering of the Nd spins) lead to a change in the conduction mechanism. In the paramagnetic-like region, the MR for both samples has a rather parabolic shape as a function of magnetization (characteristic of the scattering of charge carriers by independent spins and/or spin clusters, as found for the $n = \infty$ RP materials [38, 39]).

For both $n = \infty$ and $n = 2$ polycrystalline materials the contributions from spin-polarized tunnelling between grains or interfaces are often significant [40]. The effect of the grain boundaries has been found to be important at low temperatures and usually is reflected by a sharp drop in resistivity in low magnetic fields [41]. Furthermore, the high-field magnetoresistance can be influence by the granularity [42].

The temperature dependence of the magnetoresistance measured in 14 T for this series is plotted in figure 7(a). In contrast to the case for ferromagnetic perovskite CMR materials, where the magnetoresistance peaks at the Curie temperature, these MR values increase as the temperature decreases and reach the highest values for all samples below 100 K. This difference may result from the lack of long-range magnetic order in our $n = 2$ RP compounds but it may also indicate the involvement of tunnelling between grains or spin-dependent scattering at the grain boundaries. We shall explore the latter mechanism for the sample in which it seems most marked in the following paragraph.

Figure 6 shows that the low-field magnetoresistance of the $x = 0.2$ sample is different from that of the $x = 0.5$ sample; it drops sharply in low fields ($B < 1$ T) for the $x = 0.2$ sample and varies smoothly for the $x = 0.5$ sample. Similar behaviour of the polycrystalline layered manganites was found in the La series [43]. For the $x = 0.2$ sample we are able to separate and quantify a low-field and a high-field contribution to the magnetoresistance. The low-field magnetoresistance (LFMR) was calculated by extrapolating the $\rho(B)/\rho(0)$ dependence (figure 6) back to $B = 0$ T (see references [41, 43]) and the high-field magnetoresistance (HFMR) is calculated as the difference between the high-field resistance and the extrapolated value at $B = 0$ T.

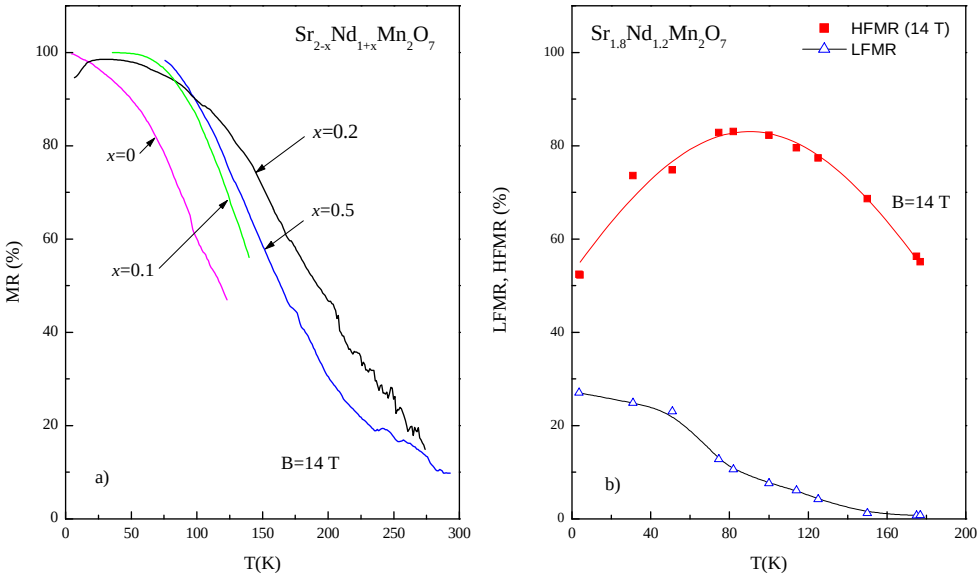

Figure 7. (a) The temperature dependence of the magnetoresistance MR $= -(\rho(T, B) - \rho(T, 0))/\rho(T, B)$ (%) in an applied field of $B = 14$ T for the series $Sr_{2-x}Nd_{1+x}Mn_2O_7$ ($x = 0$, 0.1, 0.2, 0.5). (b) The temperature dependence of the low-field (LFMR) and high-field (HFMR) contributions to the magnetoresistance of the $Sr_{1.8}Nd_{1.2}Mn_2O_7$ polycrystalline sample.

The temperature dependence of the LFMR and HFMR in 14 T of the $Sr_{1.8}Nd_{1.2}Mn_2O_7$ sample is shown in figure 7(b). The LFMR increases significantly at low temperatures and reaches a maximum of 27% at 4.2 K, which is very close to the value of 23% at 10 K obtained for the polycrystalline $Sr_{1.8}La_{1.2}Mn_2O_7$ [43]; this is likely to be due to spin-dependent transport through grain boundaries. The HFMR in 14 T is much larger than the LFMR at $T > 100$ K. The HFMR has a peak at 80 K; this temperature corresponds also to a drop in magnetization suggesting an increase of antiferromagnetic correlations (figure 4) and changes in the transport mechanism (figure 5). At the peak, the HFMR reaches values as high as 82% in 14 T and 48% in 5 T. The field dependence of the HFMR at different temperatures is almost linear, suggesting that the HFMR could be connected with the spin canting inside the grains or some other mechanism which reduces the spin fluctuations.

For the $x = 0.5$ sample we have been unable to separate the HFMR from the LFMR, since in the measured temperature range the resistivity does not drop in low magnetic fields. Similar behaviour was found in polycrystalline $Sr_2LaMn_2O_7$ [43] and was attributed to the antiferromagnetic correlations.

The fact that in our case all samples are polycrystalline with similar grain dimensions but that the LFMR was observed only for the $x = 0.2$ sample over the temperature range studied suggests that the low-field magnetoresistance may not only be a characteristic of granularity. Studies on single crystals of layered manganite $La_{1.4}Sr_{1.6}Mn_2O_7$ assigned the low-field CMR to spin-polarized tunnelling between layers [44]. This mechanism was also used to explain the anisotropic low-field magnetoresistance of the same crystal [45]. Finally, as it will be important in the analysis of the later sections, we remark that any LFMR component is very small at temperatures above 100 K. In other CMR materials [43] any contribution from inter-grain tunnelling was also very small above 100 K, which corresponds to the Curie temperature.

3.4. Magnetic clusters

The consistently high values of the resistivity across the entire temperature range at zero field and 14 T in the $Sr_{2-x}Nd_{1+x}Mn_2O_7$ series support the idea that any ferromagnetic interactions are restricted to domains of a size undetectable in previous neutron diffraction studies [28, 29]. The localized nature of the ferromagnetic interactions is underlined by the observation of diffuse scattering only at low temperature and low angle in neutron experiments for $x = 0.2$ and $x = 0.5$ [28, 29] rather than a diffraction pattern characteristic of the long-range magnetic order and enhanced magnetic moments in the other members of the $Sr_{2-x}Nd_{1+x}Mn_2O_7$ series. The regions of any ferromagnetic spin correlation may be regarded as magnetic clusters (or magnetic polarons) which are extended on application of the magnetic field when ferromagnetic spin alignment is favoured by the double exchange. Moreover, recent μSR measurements on samples similar to ours indicate the existence of magnetic clusters [46]. This likens the behaviour in our study to that observed by Blasco *et al* [47] who defined a spin-glass insulator state in their work on $La_{2/3}Ca_{1/3}Mn_{1-x}Al_xO_{3-x}$. In their study the effect of substitution for Mn with Al induces a magnetically disordered state bringing about the coexistence of metallic and insulating regions, the latter being affected by the application of a magnetic field. There is evidence that similar magnetically disordered states exist in the Sr_{2-x} $Nd_{1+x}Mn_2O_7$ series since the $x = 0$ and $x = 0.1$ compositions contain a minority spin-glass phase [16].

Comparing the MR values in 14 T for all samples at $T > 100$ K, where the magnetoresistance is predominantly HFMR (see the previous section and figure 7), we have observed that the magnetoresistance values decrease in the order $x = 0.2$, $x = 0.5$, $x = 0.1$ to $x = 0$ as the magnetization decreases. At high temperatures ($T > 100$ K), $Sr_{1.8}Nd_{1.2}Mn_2O_7$ is the most magnetoresistive and also has the largest magnetization per formula unit (figure 4), presumably due to it having the highest concentration of ferromagnetic clusters.

The dimensions of magnetically aligned clusters were determined for $Nd_{0.52}Sr_{0.48}MnO_3$ by Wagner *et al* [48] by considering that the hopping barrier depends only on the misorientation between spins at the initial and final state. Thus, in the magnetically disordered state, the change in resistivity with magnetic field scales with the square of the Brillouin function†:

$$\Delta\rho(B, T) = A(T)B_j^2(g\mu_B J(T)B/k_B T) \tag{1}$$

whereas in the ferromagnetic region the change in resistivity with magnetic field scales with a simple Brillouin function ($A(T)$ is the amplitude of the CMR). By fitting the field dependence of the resistivity at high temperatures ($T > 100$ K for $x = 0.2$), using equation (1), it is possible to determine the value of $J(T)$, which is the average spin moment in the magnetic cluster ($J = 2$ for one Mn^{3+} ion) [48]. Using this procedure and assuming that we have ferromagnetic order between the manganese ions in each cluster, we obtain the values listed in table 2. These results suggest that larger magnetoresistance is associated with samples with larger ferromagnetic clusters. The sizes of the ferromagnetic clusters increase as temperature decreases for $x = 0.5$ from $J(175\text{ K}) = 19$ to $J(77\text{ K}) = 34$ whereas for $x = 0.2$ the clusters size changes from $J(200\text{ K}) = 27$ to $J(125\text{ K}) = 31$. The magnitude of the $J(T)$ values is well correlated with the magnetoresistance values in 14 T, as seen in figure 7(a), suggesting that a possible explanation for the magnetoresistance behaviour in the intermediate-temperature range and at relatively high magnetic fields is given by the formation of magnetic clusters.

† Theoretically, the resistivity as a function of the square of Brillouin function for the $x = 0.5$ sample could be well correlated with the square of the Langevin function (as a limiting case when the $J(T)$ value is very large) and this explanation was given by Helman and Abeles [49] to describe the spin-polarized tunnelling in superparamagnetic grains.

Table 2. Fitting parameters for the field dependence of the resistivity at different temperatures and for different samples obtained by using equation (3); $J(T)$ is the average spin moment in the magnetic cluster at a temperature T.

Sample	$J(T)$	T (K)
$Sr_2HoMn_2O_7$	9.63 ± 0.01	125
$Sr_2YMn_2O_7$	9.03 ± 0.04	75
	8.64 ± 0.04	100
	7.48 ± 0.02	150
	6.85 ± 0.24	200
$Sr_{1.5}Nd_{1.5}Mn_2O_7$	34.55 ± 0.36	77
	29.08 ± 0.13	101
	25.34 ± 0.18	125
	23.70 ± 0.21	150
	19.38 ± 0.04	175
	18.56 ± 0.02	200
$Sr_{1.8}Nd_{1.2}Mn_2O_7$	31.99 ± 0.32	125
	30.34 ± 0.36	150
	29.45 ± 0.35	175
	27.63 ± 0.10	200
	25.75 ± 0.11	225

3.5. Zero-field resistivity data for the $Sr_2RMn_2O_7$ and $Sr_{2-x}Nd_{1+x}Mn_2O_7$ series

Neither Arrhenius thermally activated hopping nor the Mott variable-range-hopping (VRH) mechanism [53] describe the variation in resistivity over the entire temperature range for any of the samples studied. However, at high temperatures (above 150 K) the activation energy, E_A, extracted from $\rho = \rho_0 \exp(E_A/k_BT)$, can be estimated for all samples (table 3). Figure 8 shows that the activation energy varies almost linearly with the Jahn–Teller distortion Δ. The critical Δ value above which the samples are very insulating seems to be equal to or larger than 1.04 (see table 1). For the Y and Ho samples the values of E_A are larger than those for the Nd and Pr samples; the Y and Ho materials show more insulating behaviour, perhaps as a result of the bandwidth narrowing associated with the structural distortion.

This distortion will also weaken the magnetic coupling between bilayers as has also been observed in the layered manganite $(La_{1-z}Nd_z)_{1.2}Sr_{1.8}Mn_2O_7$ [24]. Similar results were also

Table 3. Electrical parameters obtained by considering a simple activation process ($\gamma = 1$) extracted over a relatively small temperature range (200–300 K) and a general hopping mechanism (equation (2)).

Sample	E_A (meV)	γ	T_0 (K)	Range (K)
$Sr_2PrMn_2O_7$	111.6	0.78 ± 0.12	2.88×10^3	180–300
$Sr_2YMn_2O_7$	126.6	0.70 ± 0.01	5.75×10^3	150–300
$Sr_2HoMn_2O_7$	127.9	0.70 ± 0.12	5.26×10^3	100–300
$Sr_2NdMn_2O_7$	101.1	0.65 ± 0.11	5.25×10^3	150–300
$Sr_{1.9}Nd_{1.1}Mn_2O_7$	109.5	0.72 ± 0.36	3.26×10^3	150–300
$Sr_{1.5}Nd_{1.5}Mn_2O_7$	142.5	0.75 ± 0.04	4.52×10^3	150–300

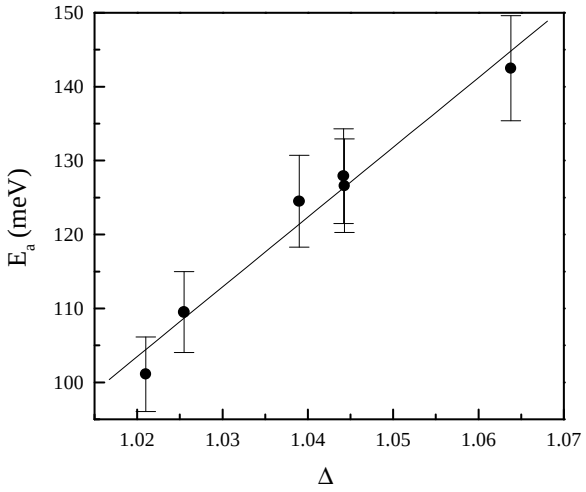

Figure 8. The activation energy E_A extracted from $\rho = \rho_0 \exp(E_A/k_B T)$ plotted as a function of the degree of Jahn–Teller distortion Δ as defined in text. In the case of biphasic materials, Δ was calculated from the average value of the bond lengths corresponding to the two $n = 2$ RP phases.

reported by Seshadi *et al* [50] on the series of compounds $Sr_{1.8}R_{1.2}Mn_2O_7$ (R = La, Pr, Nd), where the activation energy increases almost linearly with the elongation of the Mn–O apical bond as a result of doping with a smaller cation R^{3+}. These authors suggested that due to this enhanced Jahn–Teller distortion, the metal–insulator transition observed for the La compound [3] is absent for the Nd and Pr samples†.

For several perovskite CMR materials, the high-temperature region of resistivity may usually be described by a three-dimensional VRH [52]. The carrier localization length [53] obtained at high temperatures for our samples by considering an approach similar to that used by Wagner *et al* [37, 48] for perovskite materials gave values in the range 6.4 Å–13.4 Å. These values suggest a strong localization in the (a, b) plane within 1.5–3 unit cells. If we consider that the conduction takes place mainly in (a, b) planes then a possible mechanism in our rather insulating compounds could be variable-range hopping.

We have considered a general VRH mechanism [53] described by the following formula:

$$\rho = \rho_0 \exp(T_0/T)^{\gamma}. \tag{2}$$

The exponent γ is obtained from the slope of $\log W$ versus $\log T$ (figure 9), where $W = -\mathrm{d}(\ln \rho)/\mathrm{d}(\ln T)$ is the reduced activation energy [54]. The value of T_0 is expressed by the relation $T_0 = (10^a/\gamma)^{\gamma}$ where a is the value of $\log W$ when $\log T \to 0$. The extracted values of γ and T_0 as well as the fitted temperature range are given in table 3. The characteristic T_0-values vary slightly from one compound to another and are of the order of thousands of kelvins. The values of γ are distributed in the range $\gamma = 0.6$–0.8 and they are much larger than those expected for a three-dimensional ($\gamma = 0.25$) or two-dimensional ($\gamma = 0.33$) VRH‡. A study of the superconducting single crystal $PrBaCu_3O_7$ [55] showed that in the insulating region there is a strong anisotropy of the resistivity which follows an expression $\rho_c/\rho_{ab} = a + b/T^{2/3}$,

† This trend is supported by recent studies on the different composition $Sr_{1.6}R_{1.4}Mn_2O_7$ (R = La, Nd, Pr, Gd) [51] which showed the presence of a metal–insulator transition for the first three samples both in zero and applied magnetic fields but not for the latter.

‡ A similar exponent ($\gamma = 0.77$) was found in the temperature dependence of the resistivity of amorphous nickel–silicon films [55]. This was associated with a soft gap in the density-of-states variable-range hopping. A hard gap is considered for an activated T^{-1}-resistivity.

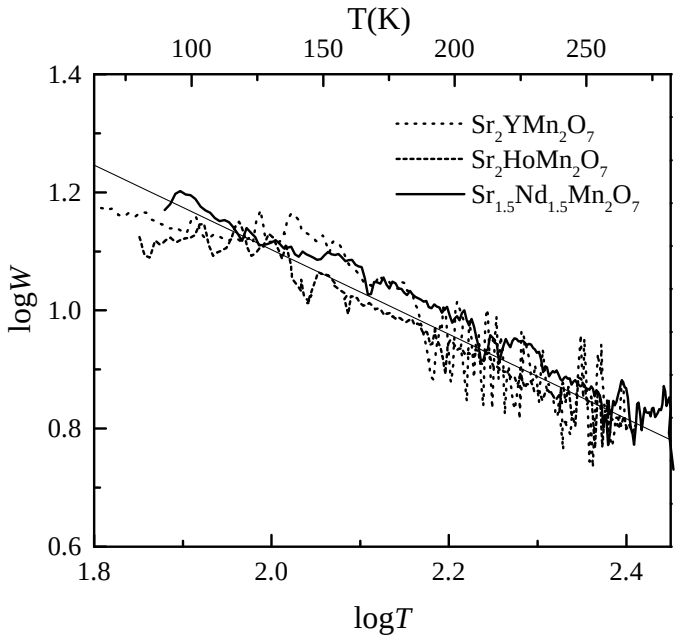

Figure 9. A log–log plot of the activation energy $W = -\mathrm{d}(\ln \rho)/\mathrm{d}(\ln T)$ versus temperature. The slope of the solid-line fit gives the exponent γ as defined in equation (1).

perhaps due to a strong localization of the carriers in the planes. Large anisotropy and strong temperature dependence between the in-plane and out-of-plane components of resistivity have already been observed in single crystals of $La_{1.4}Sr_{1.6}Mn_2O_7$ [44]. Wave functions of the localized states are spread across several unit cells in the (a, b) plane and confined to a single bilayer along the c-direction. A similar mechanism could be operating in our layered RP materials where the conduction is mainly determined by the hopping of carriers confined to bilayers. In figure 10 we present for some of our compounds the temperature dependence of the resistivity when a general hopping mechanism is considered with different values of γ. It is observed that the best fit is obtained when $\gamma = 0.66$. The values of γ obtained for our polycrystalline layered materials could reflect a $T^{-2/3}$-dependence of the resistivity as observed for the layered cuprate [55].

The significance for the magnetotransport behaviour of the presence of two $n = 2$ RP phases for $Sr_2NdMn_2O_7$ and $Sr_2PrMn_2O_7$ or one $n = 2$ RP combined with one $n = \infty$ phase for $Sr_{1.8}Nd_{1.2}Mn_2$, $Sr_2HoMn_2O_7$ and $Sr_2YMn_2O_7$ is as yet unclear. A recent high-resolution transmission electron microscopy (HRTEM) study [56] has shown that it is important to differentiate between bulk and surface homogeneity when considering phase purity in polycrystalline samples. Using neutrons ($\lambda \sim 1.5$ Å), the average bulk of the grains is probed, whereas HRTEM monitors defects or intergrowths occurring in relatively thin crystallites at or close to the surface in larger particles; intergrowths with $n \geqslant 5$ (essentially perovskite microdomains) were present in each of the compositions $Sr_2RMn_2O_7$ (R = Nd, Ho and Y). This was particularly surprising for the $Sr_2NdMn_2O_7$ phase since no higher n RP phases had been detected in the neutron study. It is likely that the defects were too small to give a coherent diffraction pattern at 1.5 Å. However, it should be noted that even disordered crystallites which contain defects or intergrowths have 95% volume fraction of unperturbed $n = 2$ structure, so the concentration of defects is fairly small.

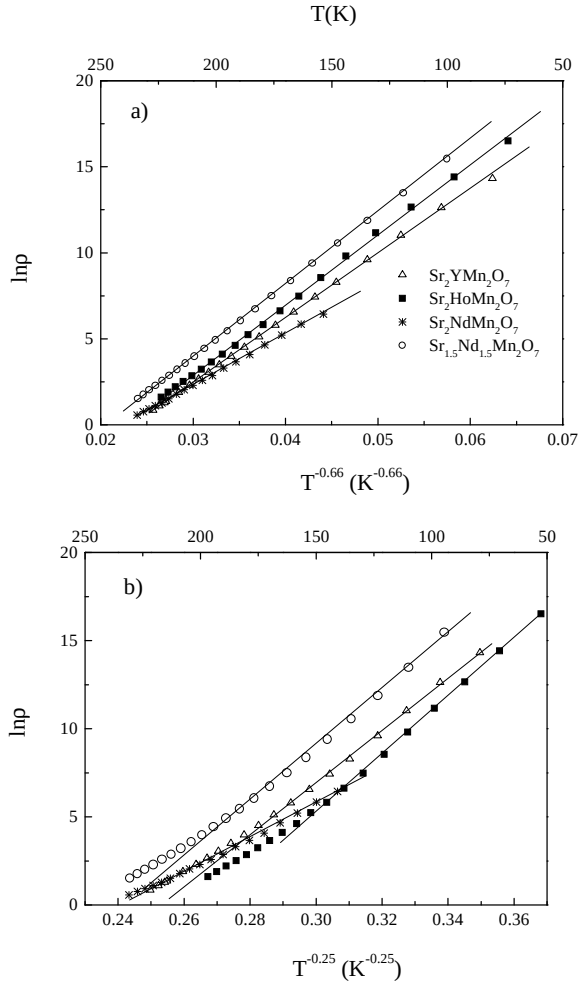

Figure 10. The temperature dependence of the resistivity $\rho = \rho_0 \exp(T_0/T)^{\gamma}$ when a variable-range hopping is considered. (a) $\gamma = 0.66$ and (b) $\gamma = 0.25$.

4. Summary and conclusions

Changing the size of the lanthanide ions across the $Sr_2RMn_2O_7$ (R = Pr, Nd, Y, Ho) series has a strong influence on the magnetotransport properties of layered compounds as is also found for $n = \infty$ perovskite [6]. The $Sr_2PrMn_2O_7$ and $Sr_2NdMn_2O_7$ compounds show distinctly different behaviour to the pair of compounds containing the smaller lanthanide ions, $Sr_2HoMn_2O_7$ and $Sr_2YMn_2O_7$. These observations suggest that once the radius of R^{3+} has reached a critically low value, CMR no longer occurs and the resistivity remains activated throughout the entire temperature range. The temperature dependence of the magnetization for Ho and Y samples also suggests a paramagnetic-like behaviour at high temperatures with a spin-glass behaviour at low temperatures. These observations are clearly different from the magnetic and electrical measurements on Pr and Nd samples where we find a complex magnetic and transport behaviour, as well as CMR. In contrast to the case for the majority of Mn perovskites showing CMR, where the largest magnetoresistive effect usually appears

around the metal–insulator transition, the magnetoresistance values of the compounds studied here continue to increase as the temperature is reduced. The magnetoresistance values in 14 T are under 40% for R = Ho and R = Y at the lowest temperature (∼75 K) whereas for the other samples the magnetoresistance is larger than 80% below 150 K.

Another factor determining the absence of CMR in the Ho and Y compounds is the elongation of the Jahn–Teller-distorted apical Mn–O bond. This effect is reflected in the activation energy of resistivity which varies almost linearly with the degree of Jahn–Teller distortion Δ. The large elongation of the out-of-plane Mn–O bond lengths leads to a narrowing of the Mn 3d bandwidth. Therefore, beyond a critical degree of distortion involving the tilting of the MnO_6 octahedra comprising the bilayers, it appears that the Mn 3d bandwidth reduces, favouring charge localization. Furthermore, the resistivity behaviour for all of the samples studied suggests a two-dimensional hopping of the charge carriers in planes together with tunnelling or hopping between planes (see table 3).

Results on the $Sr_{2-x}Nd_{1+x}Mn_2O_7$ ($x = 0$, 0.1, 0.2, 0.5) series give information on the effects of band filling on the magnetoresistive behaviour. These samples are interesting due to their significant CMR values over a wide temperature range. Long-range antiferromagnetic order was only observed in the majority phase of the $x = 0$ and $x = 0.1$ compositions with no evidence of long-range order, whether antiferromagnetic or ferromagnetic, for the $x = 0.2$ and $x = 0.5$ compositions. This is a particularly interesting result since it shows that the evolution of ferromagnetic properties with increasing x does not occur in the Nd series, in contrast to the $Sr_{2-x}La_{1+x}Mn_2O_7$ series for which the compositions with $x = 0.2$ and $x = 0.4$ are well characterized ferromagnets, undergoing a metal–insulator transition at their Curie temperatures and having a significant magnetoresistance at this temperature [3,18]. Furthermore, the differences in magnetic properties observed between the La and Nd series might be due to differences in the strengths of the competing nearest-neighbour interactions whereas the variation of the e_g electron orbital character from $d_{x^2-y^2}$ to $d_{3z^2-r^2}$ has a significant effect on the charge transport [24].

The $Sr_{1.8}Nd_{1.2}Mn_2O_7$ compound has proven particularly interesting in the current study. It shows the largest value of the magnetoresistance between 30 K and 300 K of all of the compounds studied. At low temperatures, a large contribution to the magnetoresistance is due to the effect of granularity (low-field magnetoresistance). This system is not characterized by long-range magnetic order but we have estimated it to have the largest magnetic clusters (table 2). A good correlation exists between the size of the magnetoresistance values and the size of the magnetic clusters; the square of the Brillouin function gives a good estimate of the dimensions of these clusters but the low-field effect seen in the $x = 0.2$ sample cannot be described with this model.

Our observation of CMR in both antiferromagnetic $Sr_2NdMn_2O_7$ and $Sr_{1.9}Nd_{1.1}Mn_2O_7$ and in non-ordered $Sr_{1.8}Nd_{1.2}Mn_2O_7$ and $Sr_{1.5}Nd_{1.5}Mn_2O_7$ materials illustrates that neither long-range antiferromagnetic nor ferromagnetic order is a requirement for the CMR behaviour†. Therefore it is possible that it is the minority, spin-glass phase for the $x = 0$ and $x = 0.1$ compositions or the existence of magnetic clusters for $x = 0.2$ and $x = 0.5$ (at $T > 100$ K) that is responsible for the CMR in these compositions. The lack of pure single-phase materials in some cases makes it difficult to separate different effects. It is supposed that in each case the $n = 2$ RP (∼95%) bulk phase is responsible for the CMR effect. However, the significance of the minority $n = \infty$ phase (<7%) and its effect on magnetotransport behaviour needs further investigation.

† A similar effect was observed in the case of the $n = \infty$ perovskite $(Tb_{1/3}La_{2/3})_{2/3}Ca_{1/3}MnO_3$ which shows CMR without bulk ferromagnetism [57].

Acknowledgments

This work was supported by the EPSRC. AIC would like to thank the University of Oxford and ORS for financial support. We thank P D Battle, M J Rosseinsky, J F Vente and J E Millburn for the provision of samples and fruitful discussions. We also thank B Lovett for building the magnetometer used for the high-field magnetization measurements. We are grateful to A Husmann for reading the manuscript.

References

[1] Battle P D, Blundell S J, Green M A, Hayes W, Honold M M, Klehe A K, Laskey N S, Millburn J E, Murphy L E, Rosseinsky M J, Samarin N A, Singleton J, Sluchanko N E, Sullivan S P and Vente J F 1996 *J. Phys.: Condens. Matter* **8** L427
[2] Asano H, Hayakawa J and Matsui J 1996 *Appl. Phys. Lett.* **68** 3638
[3] Moritomo Y, Asamitsu A, Kuwahara H and Tokura Y 1996 *Nature* **380** 141
[4] Jonker G H and Santan J H V 1950 *Physica* **16** 337
[5] von Helmolt R, Wecker J, Samwer K and Barner K 1995 *J. Magn. Magn. Mater.* **151** 411
[6] Ramirez A 1997 *J. Phys.: Condens. Matter* **6** 8171
[7] Kusters R M, Singleton J, Keen D A, McGreevy R and Hayes W 1989 *Physica* B **155** 362
[8] Gong G Q, Canedy C, Xiao G, Sun J Z, Gupta A and Gallagher W 1995 *Appl. Phys. Lett.* **67** 1783
[9] Maignan A, Simon C, Caignaert V and Raveau B 1995 *Solid State Commun.* **96** 623
[10] Levy P M 1994 *Solid State Physics* vol 47 (New York: Academic) p 367
[11] Rao C N R and Mahesh R 1997 *Curr. Opin. Solid State Mater. Sci.* **2** 32
[12] Rao C N R and Cheetham A K 1997 *Adv. Mater.* **9** 1009
[13] Subramanian M A, Toby B H, Ramirez A P, Marshall W J, Sleight A J and Kwei G H 1996 *Science* **273** 81
[14] Hwang H Y and Cheong S-W 1997 *Nature* **389** 942
[15] Ramirez A P, Cava R J and Krajewski J 1997 *Nature* **87** 268
[16] Battle P D, Green M A, Laskey N S, Milburn J E, Radaelli P G, Rosseinsky M J, Sullivan S P and Vente J F 1996 *Phys. Rev.* B **54** 15 967
[17] Zener C 1951 *Phys. Rev.* **82** 403
Anderson P W 1955 *Phys. Rev.* **100** 675
de Gennes P G 1960 *Phys. Rev.* **118** 141
[18] Kimura T, Tomioka Y, Kuwahara H, Asamitsu A, Tamura M and Tokura Y 1996 *Science* **274** 1698
[19] Millis A J, Littlewood P B and Shraiman B 1995 *Phys. Rev. Lett.* **74** 5144
[20] Jaime M, Hardner H T, Salamon M B, Rubinstein M, Dorsey P and Emin D 1997 *Phys. Rev. Lett.* **78** 951
[21] de Teresa J M, Ibarra M R, Algarabel P A, Ritter C, Marquina C, Blasco J, Garcia J, Moral A D and Arnold Z 1997 *Nature* **386** 256
[22] Majumdar P and Littlewood P 1998 *Phys. Rev. Lett.* **81** 1314
[23] Chauvet O, Goglio G, Molinie P, Corraze B and Brohan L 1998 *Phys. Rev. Lett.* **81** 1102
[24] Moritomo Y, Maruyama Y, Akimoto T and Nakamura A 1997 *Phys. Rev.* B **56** R7057
[25] Argyriou D N, Mitchell J F, Radaelli P G, Bordallo H N, Medarde M and Jorgensen J D 1999 *Phys. Rev.* B **59** 8695
[26] Battle P D, Green M A, Laskey N S, Millburn J E, Radaelli P G, Murphy L E, Rosseinsky M J, Sullivan S P and Vente J F 1997 *Chem. Mater.* **9** 552
[27] Battle P D, Millburn J E, Radaelli P G, Rosseinsky M J, Sullivan S P and Vente J F 1997 *Chem. Mater.* **9** 3136
[28] Battle P D, Hepburn J A, Millburn J E, Radaelli P G, Rosseinsky M J, Spring L E and Vente J F 1997 *Chem. Mater.* **9** 3215
[29] Milburn J E 1997 *DPhil Thesis* Oxford University
[30] Battle P D, Green M A, Laskey N S, Kasmir N, Millburn J E, Spring L E, Rosseinsky M J, Sullivan S P and Vente J F 1997 *J. Mater. Chem.* **7** 977
[31] Moritomo Y, Maruyama Y, Akimoto T and Nakamura A 1998 *J. Phys. Soc. Japan* **67** 405
[32] Kawano H, Kajimoto R, Yoshizawa H, Tomioka Y, Kuwahara H and Tokura Y 1997 *Phys. Rev. Lett.* **78** 4253
[33] Moritomo Y and Itoh M 1999 *Phys. Rev.* B **59** 8789
[34] Balakrishnan G, Lees M R and Paul D M^{c}K 1997 *J. Phys.: Condens. Matter* **9** L471
[35] Spring L E 1999 *DPhil Thesis* Oxford University
[36] Tokunaga M, Miura N, Tomioka Y and Tokura Y 1998 *Phys. Rev.* B **57** 5259

[37] Wagner P H, Metlushko V, Trappeniers L, Vantomme A, Vanacken J, Kido G, Moshchalkov V V and Bruynseraede Y 1997 *Phys. Rev.* B **55** 3699
[38] Furukawa N 1994 *J. Phys. Soc. Japan* **63** 3214
[39] Fontcuberta J, Martinez B, Seffar A, Pinol S, Garcia-Munoz J L and Obradors X 1996 *Phys. Rev. Lett.* **76** 1122
[40] Hwang H Y, Cheong S-W, Ong N P and Batlogg B 1996 *Phys. Rev. Lett.* **77** 2041
[41] Balcells L L, Fontcuberta J, Martinez B and Obradors X 1998 *J. Phys.: Condens. Matter* **10** 1883
[42] Balcells L L, Fontcuberta J, Martinez B and Obradors X 1998 *Phys. Rev. Lett.* **58** R14 697
[43] Dörr K, Müller K-H, Ruck K, Krabbes G and Schultz L 1999 *J. Appl. Phys.* **85** 5420
[44] Kimura T, Asamitsu A, Tomioka Y and Tokura Y 1997 *Phys. Rev. Lett.* **79** 3720
[45] Perring T G, Aeppli G, Kimura Y, Tokura Y and Adams M A 1998 *Phys. Rev.* B **58** R14 693
[46] Bewley R I, Blundell S J, Lovett B W, Jestädt Th, Pratt F L, Chow K H, Hayes W, Battle P D, Green M A, Millburn J E, Rosseinsky M J, Spring L E and Vente J F 1999 *Phys. Rev.* B at press
[47] Blasco J, Garcia J, de Teresa J M, Perez J, Algarabel P A and Marquina C 1997 *Phys. Rev.* B **55** 8905
[48] Wagner P, Gordon I, Trappeniers L, Vanacken J, Herlach F, Moshchalkov V V and Bruynseraede Y 1998 *Phys. Rev. Lett.* **81** 3980
[49] Helman J S and Abeles B 1976 *Phys. Rev. Lett.* **37** 1429
[50] Seshadi R, Martin C, Maignan A, Hervieu M, Raveau B and Rao C N R 1996 *J. Mater. Chem.* **6** 1585
[51] Hur N H, Kim J-T, Yoo K H, Park Y K, Park J C, Chi E O and Kon Y U 1998 *Phys. Rev.* B **57** 10 740
[52] Coey J M D, Viret M and Ranno L 1995 *Phys. Rev. Lett.* **75** 3910
[53] Mott N F and Davis E A 1979 *Electronic Processes in Noncrystalline Materials* (Oxford: Clarendon)
[54] Lien N and Rosenbaum R 1997 *Phys. Rev.* B **56** 14 960
[55] Levin G A, Stein T, Almasan C C, Han S H, Gajewski D A and Maple M B 1998 *Phys. Rev. Lett.* **80** 841
[56] Sloan J, Battle P D, Green M A, Rosseinsky M J and Vente J F 1998 *J. Solid State Chem.* **138** 135
[57] de Teresa J, Ibarra M, Garcia J, Algarabel P A, Ritter C, Marquina C, Blasco J, Garcia J and Moral A 1996 *Phys. Rev. Lett.* **76** 3392